Metamaterial-Inspired Vacuum Electron Devices and Accelerators

Zhaoyun Duan, *Senior Member, IEEE*, Michael A. Shapiro, *Senior Member, IEEE*, Edl Schamiloglu, *Fellow, IEEE*, Nader Behdad, *Fellow, IEEE*, Yubin Gong, *Member, IEEE*, John H. Booske, *Fellow, IEEE*, B. N. Basu, *Member, IEEE*, and Richard J. Temkin, *Life Fellow, IEEE*

***Abstract*—Metamaterials (MTMs) are structured materials with subwavelength features that can be engineered to have some unique properties not found in nature, such as negative refractive index, reversed Doppler effect, and reversed Cherenkov radiation. Based on these novel MTMs, several important research groups have made great attempts to develop novel MTM-inspired vacuum electron devices (VEDs) and accelerators. Just as solid-state power devices are innovated by incessant emerging of new semiconductor materials, VEDs can also be inspired by MTMs to have very remarkable advantages, such as smaller size, higher power, higher efficiency, and/or larger gain relative to conventional VEDs, such as traveling-wave tubes, backward-wave oscillators, and klystrons. Similarly, relative to conventional accelerators, MTM-inspired accelerators have obvious advantages, such as smaller size and higher accelerating gradient. Furthermore, MTM-inspired devices have promising applications in areas such as radar, communication, electronic warfare, microwave heating, and imaging.**

***Index Terms*—Accelerators, amplifiers, electromagnetic metamaterials (MTMs), high-power microwaves, oscillators, vacuum electron devices (VEDs).**

Manuscript received July 1, 2018; revised September 28, 2018; accepted October 20, 2018. Date of publication November 26, 2018; date of current version December 24, 2018. This work was supported in part by the National Natural Science Foundation of China under Grant 61871095, Grant 61471091, and Grant 61531010 (UESTC), in part by AFOSR MURI under Grant FA9550-12-1-0489 (MIT and UNM), in part by DOE High Energy Physics under Grant DE-SC0015566 (MIT), and in part by AFOSR under Grant FA9550-16-1-0509 (UWM). The review of this paper was arranged by Editor D. K. Abe. *(Corresponding author: Zhaoyun Duan.)*

Z. Duan and Y. Gong are with the School of Electronic Science and Engineering, University of Electronic Science and Technology of China, Chengdu 610054, China (e-mail: zhyduan@uestc.edu.cn; ybgong@uestc.edu.cn).

M. A. Shapiro and R. J. Temkin are with the Plasma Science and Fusion Center, Massachusetts Institute of Technology, Cambridge, MA 02139 USA (e-mail: shapiro@psfc.mit.edu; temkin@mit.edu).

E. Schamiloglu is with the Department of Electrical and Computer Engineering, University of New Mexico, Albuquerque, NM 87131 USA (e-mail: edls@unm.edu).

N. Behdad and J. H. Booske are with the Department of Electrical and Computer Engineering, University of Wisconsin–Madison, Madison, WI 53706 USA (e-mail: behdad@wisc.edu; jhbooske@wisc.edu).

B. N. Basu was with the Centre of Research in Microwave Tubes, IIT-BHU, Varanasi 221005, India. He is now with the Supreme Knowledge Foundation Group of Institutions, Mankundu 712139, India (e-mail: bnbasu.india@gmail.com).

Color versions of one or more of the figures in this paper are available online at http://ieeexplore.ieee.org.

Digital Object Identifier 10.1109/TED.2018.2878242

I. Introduction

In 1967, Veselago [1] theoretically investigated the exotic electromagnetic properties such as negative refractive index, reversed Doppler effect, and reversed Cherenkov radiation (RCR) in an assumed homogeneous isotropic electromagnetic material in which the real parts of permittivity and permeability are both negative. Veselago [1] referred to this material as a "left-handed medium (LHM)," which has subwavelength features that are engineered to have some unique properties not generally found in nature. More than 30 years later, such materials began to receive much attention. Pendry *et al.* [2], [3] theoretically analyzed the negative permittivity of a regular array of conducting wires [2] and the negative permeability of a split-ring resonator (SRR) array [3]; they also predicted the possibility of realizing an LHM. Smith *et al.* [4] followed the work of Pendry *et al.* [2], [3] and constructed an LHM for the first time. Afterward, negative refractive index at the boundary of an LHM and vacuum was demonstrated in experiment [5]. Subsequently, the unusual electromagnetic properties of the reversed Doppler effect [6] and RCR [7]–[9] were experimentally verified. Since then, the LHM and other related types of artificial materials, now termed metamaterials (MTMs), have been widely studied worldwide.

The definition of MTM—the term being coined in 1999 by Walser of the University of Texas–Austin [10]—in which the Greek word "meta" means "beyond," has not been completely agreed upon. MTMs are most commonly defined to be structured materials with subwavelength features. More specifically, MTMs are composites that have a desired combination of properties which cannot be individually obtained by combining the properties of their constituents. MTMs can be formed by embedding inclusions and material components in host media, usually with a periodic arrangement of unit cells, to achieve composite media that may be engineered to have qualitatively new physically realizable response functions that do not occur or may not be easily available in nature [11]. However, the nonperiodic arrangements of the unit cells of MTMs and random MTMs have also been studied [12]. From the effective-medium theory [13], [14], MTMs can be classified as single-negative permittivity materials, single-negative permeability materials, double-negative materials (DNMs, also called LHMs), and near-zero refractive index materials. Many ideas for valuable applications of MTMs have also been proposed.

In the course of the extensive research of MTMs over the last decade, bulk MTMs have encountered significant challenges in their realization and fabrication, as well as characterization. Thus, a 2-D MTM, now called a metasurface, has been proposed by Falcone *et al.* [15], Holloway *et al.* [16], Yu *et al.* [17], Gonidec [18], Chen *et al.* [19], Khorasaninejad and Capasso [20]. A metasurface consists of a single-layer or a few-layer stacks of planar structures and can be straightforwardly fabricated using lithography, nanoprinting, or other methods. Notably, the metasurface cannot be described using an effective-medium theory that assigns an effective permittivity (ε_{eff}) and an effective permeability (μ_{eff}) to the medium, and consequently, the concept of surface impedance was introduced for its description [19]. Presently, metasurfaces are receiving much attention, especially, in optics [20].

The first attempt to incorporate an MTM in a vacuum electron device (VED) dates back to the year 2008 [21]. In tandem with this, a relevant breakthrough was the intensive study of RCR encompassing theory, simulation, and experiment [7]–[9], [22]–[25], especially, the first experimental observation of RCR using a pencil beam [7], [8] and using a sheet beam [9]. This study aroused tremendous global interest in the application of RCR-based MTMs in VEDs side by side with the study on the use of conventional MTM structures in VEDs such as TWTs [26]–[29], the resistive wall amplifier [30], BWOs [31], backward-wave amplifiers [32], and klystrons [33] for their performance improvement. Furthermore, an electron beam interacting with a metallic MTM slow wave structure (SWS) has been found to generate microwave radiation [34], [35].

One of the motivations for using MTMs as interaction structures is to enhance the beam–wave interaction and to improve the performance of VEDs. Due to their subwavelength property, the periodic circuits of MTM-assisted VEDs have smaller dimensional features than those of conventional VEDs. In addition, owing to the strong resonant behavior, higher interaction impedance can be obtained from MTM-assisted VEDs than from the conventional VEDs. Thus, the study of the beam–wave interaction mechanism [36] in MTM-inspired VEDs predicted higher powers, higher electronic efficiencies, and/or larger gains, and miniaturization [37].

In addition, the MTM filling of cavities has been used to increase the phase velocity and wavelength in the cavity gap, thereby making it possible to increase significantly the diameter of a multibeam klystron (MBK) allowing a greater number of electron beams to pass through the cavities. This can yield a higher total beam current and, consequently, a larger output power from an MBK [33].

Also, the accelerating cavities assisted by MTMs can yield new accelerators that would have higher accelerating gradients and smaller size, attributable to the capability of the structure to support slow waves without using the space-consuming corrugated structures that are used in their conventional counterparts [38].

The remainder of this paper is organized as follows. In Section II, we review the recent advances in RCR, MTM-inspired VEDs, and accelerators while projecting some of their exciting performances. In Section III, we highlight the role of MTM assistance in improving the performance of VEDs and accelerators as well as the various challenges in implementing this improvement. We also present the conceptual and behavioral difference between the conventional periodic and MTM-assisted interaction structures. In Section IV, this paper is concluded by highlighting the advantages of MTM-inspired VEDs and accelerators over their conventional counterparts and the scope for advancing their theoretical understanding and developmental technology.

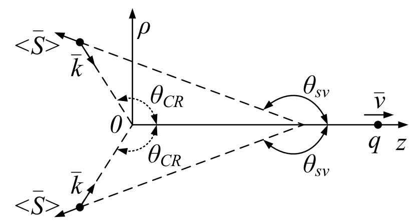

Fig. 1. Schematic of reversed Cherenkov radiation in double-negative materials.

II. Recent Advances in MTM-Inspired VEDs and Accelerators

A. Advances in Reversed Cherenkov Radiation Research

The use of MTMs as the interaction structures of Cherenkov type of VEDs, such as TWTs and BWOs, can improve the devices' performance. This opens the possibility of conceiving new RCR devices inspired by MTMs. In fact, the realizable LHM has to be anisotropic, and even bianisotropic, unlike in the prediction of RCR by Veselago [1], who had assumed the LHM to be homogeneous and isotropic. Thus, the study of RCR in an anisotropic LHM becomes quite important.

Duan *et al.* [22], [23], to the best of our knowledge, were the first to point out that for RCR in anisotropic DNMs, the wave vector and time-averaged Poynting vector are not exactly antiparallel. This is contrary to what is predicted for isotropic MTMs by Veselago [1], as explained in Fig. 1, in which the relevant quantities are as follows. q is the amount of charge of the charged particle. θ_{sv} is the angle between the time-averaged Poynting vector $\langle\bar{S}\rangle$ and the velocity $\bar{v}$ of the charged particle. θ_{CR} is the angle of the wave vector $\bar{k}$ with respect to the particle velocity $\bar{v}$. Furthermore, the directions of $\langle\bar{S}\rangle$ and $\bar{k}$ in anisotropic DNMs are nearly but not exactly antiparallel in view of θ_{CR} being not exactly equal to θ_{sv}. More details of the explanation can be found in [22]. Thus, Veselago's theory [1] was extended to a realizable LHM [39].

In order to facilitate the realization of the DNM, Duan *et al.* [24], [25] switched from the case of an infinite DNM to that of an DNM-filled waveguide. Thus, the physical properties of RCR were theoretically investigated for a single charged particle traveling along the axis of a cylindrical waveguide filled with anisotropic DNMs. The Cherenkov radiation conditions and RCR were obtained using an analytical method. The influence of the related parameters, such as the particle velocity, the waveguide radius, and the constitutive parameters of the anisotropic DNMs on the

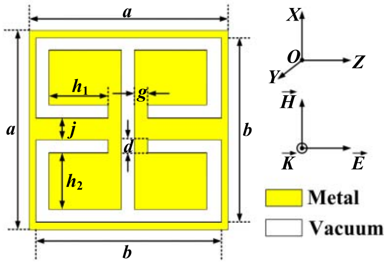

Fig. 2. Proposed unit cell of complementary electric SRR for constructing brand-new left-handed materials.

RCR was discussed. Since most of the realized MTMs are anisotropic, the theoretical work based on anisotropic DNMs should be helpful for potential experimental realizations. Obviously, the intensity of the RCR was found to be rather low due to only a single charged particle (an electron) being considered in the study. Hence, to further exhibit improvements in the RCR intensity, an electron beam rather than a single electron was used to greatly enhance the RCR [40]. The paper [9] laid a solid foundation for an RCR experiment in 2017.

With the development of terahertz (THz) science and technology, suitable THz sources are imperative. This prompted Duan *et al.* [41] to theoretically investigate electromagnetic radiation excited by a charged particle moving along a semi-infinite space filled with a DNM. RCR in the double-negative region exhibits backward radiation. The surface wave in the vacuum region was also investigated. They concluded that the amplitude of the surface wave can be greatly enhanced up to 100–1000 times the amplitude available from conventional dielectric-material devices [41]. The enhanced surface wave [42] may be useful for high-frequency and high-power VEDs assisted by DNM.

In 2014, Duan *et al.* [39] proposed an all-metal complementary electric SRR (CeSRR) for realizing an LHM. The unit cell is shown in Fig. 2 [39]. (Here, $a = 14.5$ mm, $b = 13.5$ mm, $d = 1$ mm, $j = 1.5$ mm, $h_1 = 4.25$ mm, $h_2 = 4$ mm, $g = 1$ mm, and thickness $t = 1$ mm that is not shown.) ε_{eff} and μ_{eff} are retrieved by using the S-parameters of the CeSRR. Subsequently, the dispersion relation of a waveguide loaded with CeSRRs was obtained [39]. The work paved the way for experimentally verifying RCR [9].

In 2017, based on the realized LHM with CeSRRs [39], which is suitable for observing RCR using real charged particles, the experimental scheme was proposed, as shown in Fig. 3 [9]. Duan *et al.* [9] demonstrated that this MTM exhibits left-handed behavior. They also experimentally observed Cherenkov radiation emitted predominantly in a direction nearly opposite to that of the movement of a single sheet electron beam bunch. Thus, the unusual RCR was experimentally observed for the first time. More details can be found in [9] and "supplementary information" therein. This experimental work greatly advances research in RCR-based VEDs.

B. MTM-Inspired Oscillators

The Massachusetts Institute of Technology (MIT) research group and collaborators in 2012 analyzed the possibility of an electron beam interacting with a negative-index MTM with the aim of designing either a high-power microwave device or a particle accelerator [43]. They recognized the necessity of providing metallic plates to form the MTM which can be made to interact with an electron beam, since the usual substrates supporting split-ring MTM designs do not work in ultrahigh vacuum. A similar conclusion was also reached earlier by Shiffler *et al.* [44]. A complete practical design of the MIT experiment was completed and published in 2014 [31]. The resulting experimental setup is shown in Fig. 4 [45]. The MIT experiments were conducted using a modest current electron beam passing through an MTM-loaded waveguide.

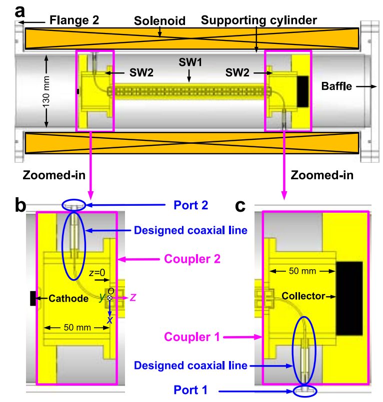

Fig. 3. Schematic of observing reversed Cherenkov radiation. (a) CeSRR layer with two couplers located in the center of the SW1 that is covered by a solenoid. (b) Zoomed-in section of Coupler 2. (c) Zoomed-in section of Coupler 1.

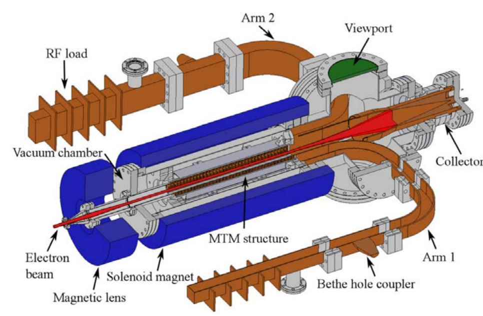

Fig. 4. MIT experimental setup.

In stage-I of the experiments, power levels of up to 5 MW were observed in backward-wave modes at a frequency of 2.40 GHz using a 1-μs pulsed electron beam of 490 keV, 84 A in a 400 G magnetic field [8]. This was the first experimental demonstration of high-power microwave emission from an electron beam interacting with an MTM structure. The output power was expected in a Cherenkov backward-wave mode satisfying the condition $\omega - k_z v_z = 0$, where ω is the emission frequency, k_z is the axial wavenumber, and v_z is the axial velocity. However, contrary to all previous theoretical predictions and the limited prior experimental experience, the output power was not generated in the Cherenkov mode. Instead, the presence of the magnetic field induced a Cherenkov-cyclotron (or anomalous Doppler) instability, satisfying the condition $\omega = k_z v_z - \Omega_c/\gamma$, where $\Omega_c = eB_z/m$

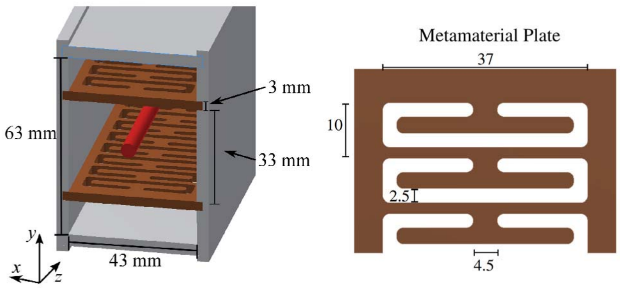

(a) (b)

Fig. 5. (a) Schematic of the MTM backward-wave oscillator and (b) one period of the MTM plate. The electron beam is shown in the waveguide in red.

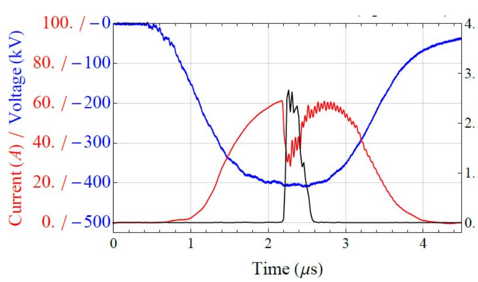

Fig. 6. Microwave power measured at the microwave output couplers (black) with the scale on the right. In addition, the measured gun voltage (blue) and collector current (red) are shown with the scale for both on the left.

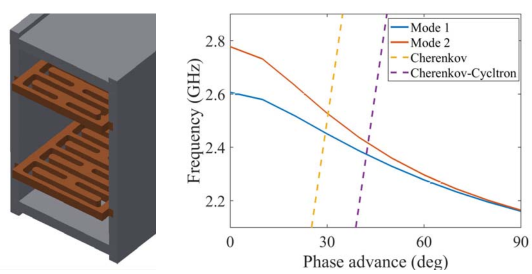

(a) (b)

Fig. 7. MTM-R circuit design. (a) Geometry. (b) Dispersion curves. The Cherenkov-cyclotron synchronism is calculated for a 490-kV beam with a magnetic field of 400 G.

is the cyclotron angular frequency, and γ is the Lorentz factor. The uniqueness of this result was described in [46].

In Fig. 5, a schematic of the MTM plates and the MTM waveguide used in the stage-I experiments are shown [8]. The waveguide is created by inserting two MTM plates loaded with periodic arrays of complementary SRRs (CSRRs). CSRRs were first proposed in [15] and are the electric analogs of SRRs. The plates are 3.175 mm thick, the period of the CSRRs is 10 mm, the spacing between the MTM plates is 29 mm, and the overall length of the structure is 370 mm.

Fig. 6 shows the microwave signal of about 350 ns in duration and a peak power of about 2 MW [8]. The gun voltage and current measured at the collector are also shown. When the microwave device starts up, a significant amount of beam interception is observed, as evidenced by the dip in the collector current. This current striking the thick MTM plates over an extended length did not induce any visible damage in the plates.

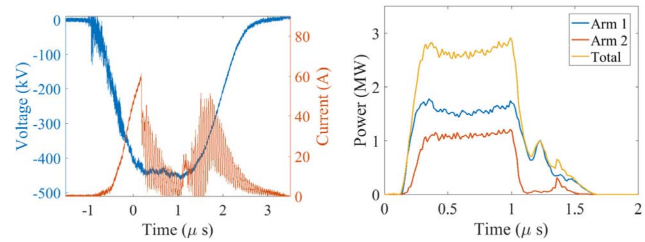

(a) (b)

Fig. 8. Sample pulse with the steering coil current applied. (a) Gun voltage and collector current. (b) Output microwave power.

The stage-II experimental results based on the MTM plates in the "MTM-R" configuration are presented in [45]. The difference in the stage-II circuit design from the stage-I design in [8] is that one of the MTM plates is reversed, as can be seen in the schematic of the MTM waveguide (Fig. 7(a), see [45]). In this way, the electron beam sees a deflecting mode as the fundamental mode. The waveguide length is 370 mm, and the plates are separated from each other by 32 mm. The electron beam travels between the two plates along the centerline of the waveguide. The CSRRs (C-shaped cuts) have a period of 10 mm, and on the two plates, the C shapes are aligned in opposite directions, i.e., reversed, hence, the name MTM-R.

The dispersion curves of the lowest two modes are shown in Fig. 7(b), labeled as Mode 1 and Mode 2 [45]. Both of them are hybrid deflecting modes with a negative group velocity. Again, there are two types of possible interaction mechanisms with the beam: the Cherenkov type interaction with the dispersion of $\omega = k_z v_z$ and the Cherenkov-cyclotron type interaction with the dispersion of $\omega = k_z v_z - \Omega_c/\gamma$. The most intense interaction was expected to be the Cherenkov-cyclotron type with Mode 1 at 2.4 GHz. The generated power is coupled out into two WR284 waveguides assembled at the end of the MTM waveguide.

A magnetic lens and pair of steering coils close to the gun, and a solenoid magnet in the MTM structure region was used to confine and control the beam. Power generated in the two output ports was guided into two waveguides and measured through a calibrated Bethe-hole coupler with a power meter and a fast oscilloscope. A group of frequency filters was utilized with the power measurement to make sure that the measured power was in the design mode. A large parameter space of different values of the lens field, solenoid field, and beam voltage (current) were tested. A pair of steering coils allowed one to manipulate the beam in the transverse direction. When the beam gains a transverse velocity from the steering coils and enters the solenoid region with a longitudinal magnetic field, the cyclotron motion is started. Since the microwave field between the two plates can be viewed as a superposition of the two surface waves concentrated on the two MTM plates, pushing the electron beam closer to one of the plates can potentially improve the output power. In fact, a greatly improved operation was obtained in stage-II experiments. An example of an improved pulse is shown in Fig. 8 [45]. The beam voltage is 420 kV, and the gun current is 60 A. The collector current drops quickly to almost zero due to the onset of the Cherenkov-cyclotron deflecting mode with a transverse electric field. The missing collector current is intercepted by the MTM-R structure. However, there was no evidence of arcing or damage to the MTM plates. The total output power was 2.9 MW with a full 1-μs pulsewidth and an efficiency of 10%. The operating lens field was 725 G, and the solenoid field was 437 G. Once the oscillation starts, the power rises to the full value within 100 ns. The maximum peak power observed in stage-II experiments was 8 MW.

The Schamiloglu group at the University of New Mexico (UNM), Albuquerque, NM, USA, has studied the evolution of wave dispersion in systems of all metallic periodic structures with increasing corrugation depth using HFSS. Their results point out the similarity of the properties of waves in MTM SWSs and traditional metallic SWSs used in high-power microwave sources [47]. In their work it is shown that when the corrugation depth exceeds a threshold value, the lowest order mode with negative dispersion appears in the first passband, the phenomenon that was traditionally assumed to only occur in MTM SWSs. Furthermore, the appearance of the lowest order mode with negative dispersion in the first passband is accompanied by the appearance of a hybrid mode as the lowest order mode with which an electron beam interacts. This was later explained by collaborators at Louisiana State University, Baton Rouge, LA, USA. They utilized an asymptotic analysis to show that corrugated waveguides can be approximated by smooth cylindrical waveguides with effective MTM surface impedance [48]. They confirmed the Schamiloglu group's hypothesis in [47] that the threshold corrugation depth for the appearance of negative dispersion corresponds to a sign change in the imaginary part of the slot admittance. In particular, they found that the anisotropic surface admittance $\Upsilon_{ad}(k,n) = H_0^{\varphi}/E_0^z|_{r=r_m}$ changes sign at the threshold radius $r = r_m$, where r_m is the minimum radius of the waveguide [48].

In 2016, the Schamiloglu group first described a new O-type high-power microwave oscillator that uses an MTM SWS supporting waves with negative dispersion. The MTM SWS comprises a biperiodic array of alternating, oppositely oriented SRRs connected to a metal tube. The SRRs provide for negative permeability. The distance between the SRRs is much less than one wavelength of the radiation generated. The biperiodic array of SSRs is nonbianisotropic since the broadside coupling of a ring, and charge distribution does not result in a net electric dipole. Hence, there is no magnetoelectric coupling in this MTM SWS. The diameter of the metal tube is such that the generated oscillations are below the cutoff for a regular waveguide with the same dimension, thus providing negative permittivity. This O-type MTM SWS is a double negative.

A tubular electron beam propagates coaxially within this structure. The interaction space is coupled with the outer coaxial channel through gaps between the SRRs. Radiation is extracted in an endfire manner at the output end of the outer channel via a conical horn section. Particle-in-cell (PIC) simulations using MAGIC [49] show that the electron beam in the interaction space forms a sequence of trapped electron bunches by the synchronous operating wave. The applied beam and magnetic field parameters are: beam voltage $U = 400$ kV,

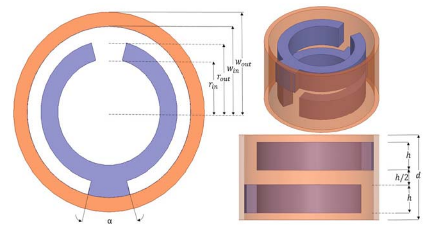

(a)

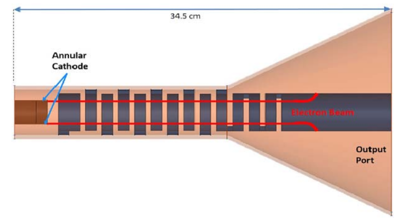

(b)

Fig. 9. (a) Geometry of the O-type MTM SWS in different perspectives for a single unit cell comprising two oppositely oriented SRRs. (b) Illustration of the entire SWS and extraction geometry.

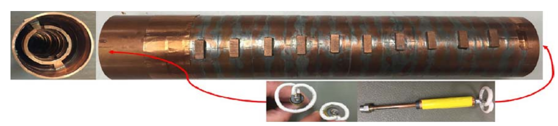

(a)

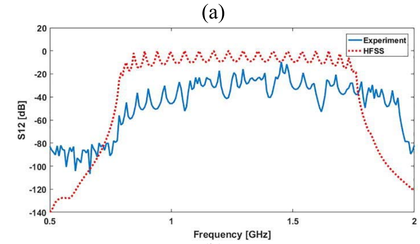

(b)

Fig. 10. (a) Experimental setup of the structure with a two-mode launcher. (b) Comparison between S_{12} measurements and HFSS simulation results of the MTM SWS.

beam current $I = 4.5$ kA, and the axial guide magnetic field $B = 2$ T. The radiation power P and radiation frequency f are 260 MW and 1.4 GHz, respectively. The electronic efficiency is 15%, and the total SWS length L is 34.5 cm. A unit cell of the O-type MTM SWS and the entire SWS comprising 12 periods of the SRRs with extraction geometry are shown in Fig. 9 [50]. The output radiation pattern corresponds to a TE_{21}-like hybrid mode.

Experimental cold tests of a crudely constructed MTM SWS were in agreement with the HFSS calculations, as shown in Fig. 10, confirming that the first passband is between 0.76 and 1.76 GHz [35].

Following a confirmation of the double-negative characteristics of this MTM SWS, a final structure was precision-machined (Fig. 11) and studied in hot tests using UNM's SINUS-6 electron beam accelerator (Fig. 12) [50]. The experimental hot test results validated the MAGIC simulations with a record output power of about 100 MW at 1.43 GHz. Fig. 13 presents the MAGIC simulation prediction of frequency together with the experimentally measured frequency.

Finally, a version with an improved reflection structure, as shown in Fig. 14, increased the efficiency to 18% with 310-MW output power [35].

Fig. 11. Photograph of a precision-machined biperiodic MTM SWS studied in hot tests.

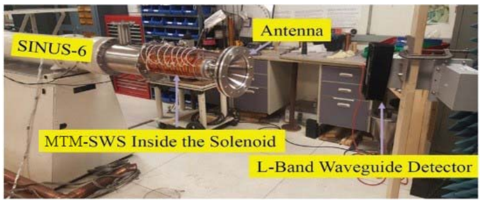

Fig. 12. Photograph of the experimental setup at UNM with critical components identified.

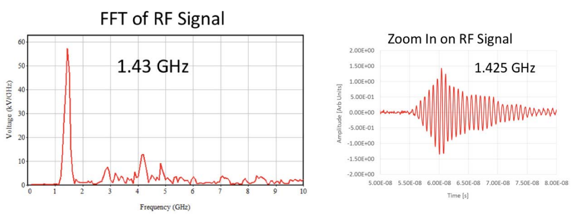

(a) (b)

Fig. 13. Comparison of the (a) frequencies predicted in MAGIC simulations with the (b) experimentally measured frequency.

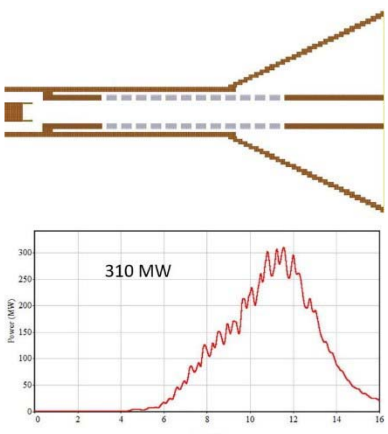

Fig. 14. Improved efficiency after optimizing the reflection of the system. Improved design of the MTM SWS (top). Radiated power (bottom).

A tremendous challenge faced by the UNM researchers was the limitation of the pulselength from their SINUS-6 accelerator. The output pulselength is about 13 ns, so it was imperative to identify the MTM SWS designs in PIC simulations that would start oscillating in a few nanoseconds and reach saturation within 13 ns. This constraint is what drove the UNM MTM SWS design.

The Duan group at University of Electronic Science and Technology of China (UESTC), developed an MTM-inspired VED based on RCR. In 2015, a novel LHM SWS [34] was proposed. The hollow circular waveguide of diameter 40 mm (Fig. 15) operating below the cutoff frequency for the TM_{11} mode can be considered as a negative permeability medium. The periodic array of the CeSRR unit cells (with its sizes given in [34]) (Fig. 15) can be treated as a negative permittivity medium. Therefore, this SWS (Fig. 15), consisting of the hollow circular waveguide and the periodic array of the CeSRR unit cells, can be regarded as an LHM for the operating frequency. More details are given in [34] and [27], the latter cited in [34]. Furthermore, this LHM SWS was suitable for a pencil electron beam to interact with and yielded an interaction impedance as high as 1200 Ω. The simulation model of an S-band RCR-based MTM BWO was built (Fig. 15), and the CST PIC simulated results predicted a peak output power of 4.0 MW at 2.454 GHz, with a relatively higher electronic efficiency of 31.5% as compared to conventional BWOs [34].

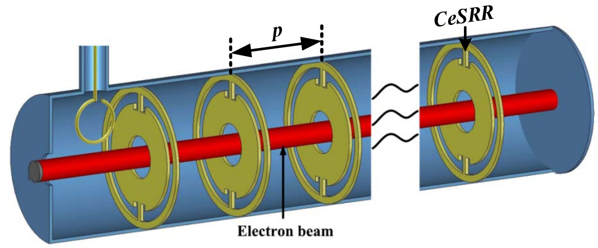

Fig. 15. PIC simulation model of an MTM backward-wave oscillator (p is the period of the CeSRR array).

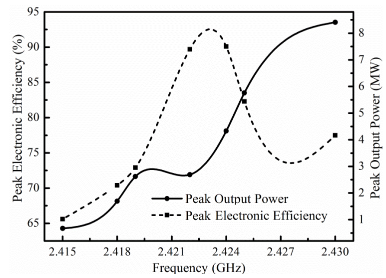

Fig. 16. Peak electronic efficiency and output power as functions of frequency.

For further improvement in device performance, the output coupler was changed from a coaxial coupler to a waveguide coupler and the period (p) is optimized [51]. The simulated results (Fig. 16) showed that the peak electronic efficiency of this S-band MTM BWO could go up to 90% with a peak output power of 4.5 MW. In other words, the averaged electronic efficiency was 45%. Notably, here, the traditional methods of beam velocity jumping or RF phase velocity tapering for beam–wave resynchronization to enhance the efficiency of O-type tubes have not been employed. Therefore, it is expected that with the incorporation of these traditional methods, the device efficiency could be further improved.

Furthermore, for the MTM which assists the VED, although it resembles the coupled-cavity SWS (CCSWS) of a TWT in shape, it is different from the CCSWS in that, for the frequencies corresponding to, say S-band, the size of the unit cell of the MTM is much smaller—thereby making it a subwavelength unit structure, unlike a CCSWS. In addition, the transverse dimensions of a conventional disk-loaded waveguide of an accelerator are comparable to the wavelength. In fact, that is why, unlike the geometry of a CCSWS or disk-loaded waveguide, the geometry of the subwavelength

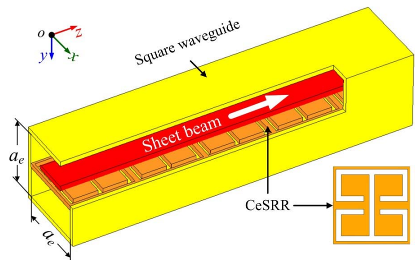

Fig. 17. Schematic of the MTM SWS with complementary electric SRR.

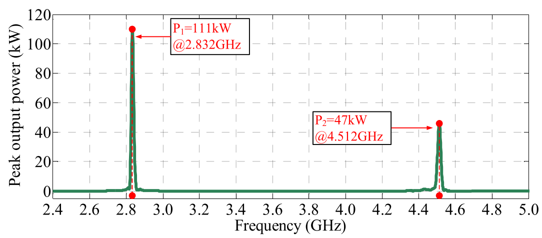

Fig. 18. Peak output powers P_1 and P_2 as functions of frequency.

MTM can be treated using an effective-medium theory. Also, the MTM provides a strong resonance, leading to a rather strong axial electric field of the surface wave. This makes the interaction impedance of this MTM much higher than that of the CCSWS. For instance, the interaction impedance of the novel MTM is from 800 to 1200 Ω at S-band, while the interaction impedance of the CCSWS is from 300 to 400 Ω (see "Supplementary Information" in [9]). The enhanced interaction impedance of the MTM in turn enhances the electronic efficiency, establishing its attractive advantage for application in narrowband VEDs.

In the meantime, another MTM with CeSRRs was developed [39]. This all-metal MTM, which is helpful for outgassing, proves to be suitable for a vacuum environment and sheet electron beam transport which was theoretically analyzed in [52]. In addition, like the MTM shown in Fig. 15, it has a rather high interaction impedance (∼800 Ω), which corresponds to a high output power and high electronic efficiency. This is because the output power is approximately proportional to the one-third index of power of the interaction impedance [36]. Therefore, the large improvement of the interaction impedance can greatly increase the output power and the electronic efficiency. These results clearly exemplify an important application of RCR to VEDs.

Based on [39], a dual-band reversed Cherenkov Oscillator using a CeSRR MTM SWS (Fig. 17) with a waveguide coupler was also developed in 2017 [53]. The simulation results show that the electronic efficiency of this dual-band oscillator can reach 52%, and its tuning bandwidths are ∼7 and ∼30 MHz for the two modes labeled as 1 and 2, respectively. It is also found that the peak output power for mode 1 (P_1) is ∼111 kW at 2.832 GHz and that for mode 2 (P_2) is ∼47 kW at 4.512 GHz [53], as shown in Fig. 18. That the device with only a single MTM structure can operate in two bands at the same time establishes an amazing merit of the MTM structure. This is an advantage since the conventional methods make it difficult to realize two bands using only a single SWS [53], and thus, this adds another virtue of MTM-inspired devices.

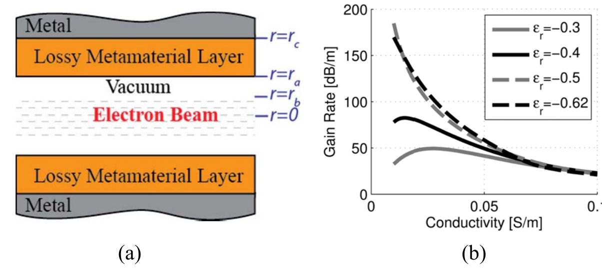

Fig. 19. Cross-sectional view of an MTM enhanced resistive-wall amplifier that uses a (a) lossy epsilon-negative MTM and (b) gain of the MTM enhanced resistive-wall amplifier versus the conductivity of the resistive medium for different relative permittivity values of the MTM.

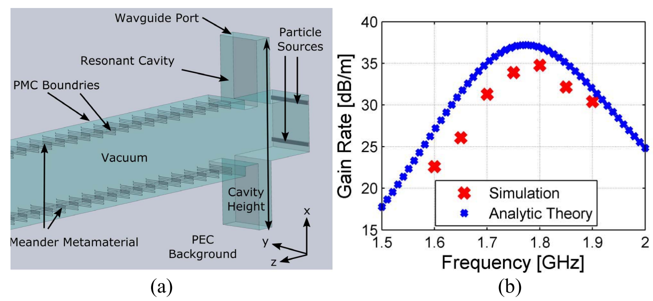

Fig. 20. (a) Practical parallel-plate MTM enhanced resistive-wall amplifier model constructed in CST Particle Studio and (b) its simulated and analytic gain rates versus frequency.

Furthermore, this novel MTM SWS enjoys a miniaturized size ∼λ/7–∼λ/5 compared to the size ∼λ/3–∼λ of its conventional counterparts, for instance, of a BWO [9]. (Here, λ is the free-space wavelength.) For example, the diameter of the SWS is about λ [54], while the size of the cross section of the SWS [9] used in an MTM-inspired device is about $\lambda/6$. These findings as well as those with respect to the MTM-inspired oscillators [51] clearly establish that the MTM-inspired oscillators have a smaller size, higher power, and higher efficiency.

C. MTM-Inspired Amplifiers

The Booske–Behdad group at the University of Wisconsin–Madison (UWM), WI, USA, first proposed the MTM enhanced resistive-wall amplifiers (ME-RWAs) in 2015 [30]. They studied the ME-RWA using a lossless epsilon-negative (ENG) MTM support medium and a resistive layer. The theoretical prediction shows that extremely high gain rate values exceeding 100 dB/m can be obtained using ENG MTM layers as the support medium of the resistive layer in an RWA. Furthermore, the model of the ME-RWA using a lossy ENG MTM was proposed and is presented in Fig. 19(a). Fig. 19(b) shows the gain rate of the single-layer ME-RWA versus conductivity for different permittivity values of the lossy MTM layer. It can be found that the maximum gain rate of the device increases with a more negative permittivity value until a specific permittivity value is reached.

In 2016, they reported the results of investigating into practical MTM implementations with approximate Drude-type responses that enable the realization of an ME-RWA [55]. They used the CST Particle Studio to conduct PIC simulations of the parallel-plate configuration of the ME-RWA, as shown in Fig. 20(a). Then, they modified the previous

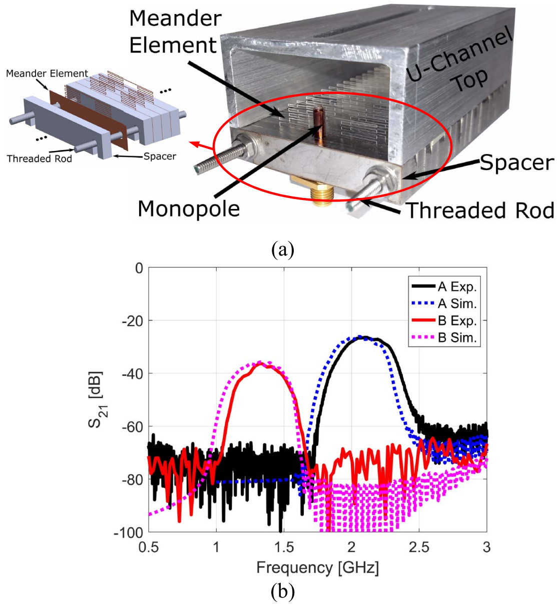

Fig. 21. (a) Assembled MTM periodic structure and (b) its transmission coefficient versus frequency.

theoretical model [Fig. 19(a)], which used an electron beam that was on-axis and axis-symmetric, and its current density and thickness were set to be the same as in the simulation. The results presented in Fig. 20(b) demonstrate that the modified theoretical results show good agreement with the PIC simulated results. Note that, the liner loss is greater than necessary in the simulations to ensure the stability. The gain rate increases if the liner loss is decreased. However, if the liner loss decreases too much, the backward-wave instability will arise. Therefore, it is also possible to increase the current density of the electron beam to increase the gain rate.

Based on the above-mentioned work, they reported a periodic arrangement of inductive meandered lines, which can be used as another practical MTM implementation, in 2017 [56]. The assumed MTM periodic structure and its transmission coefficient are presented in Fig. 21(a) and (b), respectively. When placed along the bottom of a rectangular waveguide, this MTM implementation was demonstrated to successfully emulate an epsilon-negative liner through both transmission and dispersion measurements. In Fig. 21(b), there is a frequency shift in the passband between meander sets A and B. The frequency shift between the two meander sets is due to the different meander dimensions. Meander set B used 15-mm-wide meanders whereas set A used 10-mm-wide meanders. The theoretical analysis and experimental results show that the desired passband of MTM can be achieved by selecting the meander dimensions and the required power absorption coefficient can be obtained by selecting a metal with the appropriate conductivity. This all-metal MTM periodic structure has potential applications in VEDs.

The Basu group at the Supreme Knowledge Foundation Group of Institutions, CEERI, and MTRDC [27], [29], [57] is engaged in improving their work on LHM-loaded helix SWS by taking into account the frequency dependence of LHM parameters. They are also probing into the potential

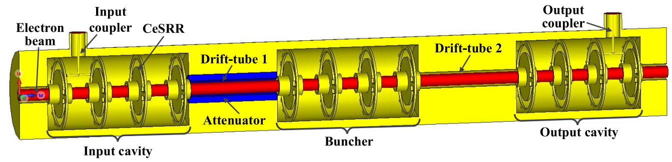

Fig. 22. Schematic of the MTM-inspired EIK.

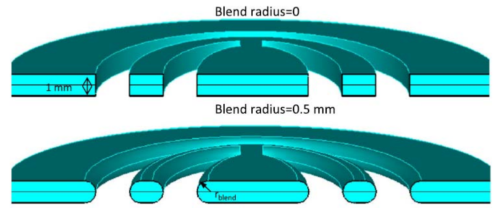

Fig. 23. Cross section of the complementary SRR used in the deflecting cavity with rectangular conductors (top) and edges smoothed with a blend radius of 0.5 mm (bottom).

of the structure in multiple bands of frequencies without requiring any alteration in the helix and the structure envelope dimensions, contrary to the use of the other conventional structures used individually in different bands of frequencies.

Galyamin *et al.* [58] from the St. Petersburg State University, Saint Petersburg, Russia, pointed out that the transition radiation (TR) excited by a charge crossing an LHM boundary has a relatively large magnitude relative to ordinary TR. Furthermore, the TR in a waveguide partly filled with an LHM has been reported [59]. Based on the unusual TR, the Duan group at UESTC began to study the novel MTM-inspired TR from 2016 [60]. They have proposed the MTM-inspired extended interaction klystron (EIK), as shown in Fig. 22. The cross section (only 40 mm diameter) of the structure of the device is smaller than that of the conventional klystron (by the order of ~1/3–~2/3) [61]. Taking typically the beam voltage and current 33.5 kV and 4 A, respectively, the axial uniform guide magnetic field 2000 G, and the input power 1.6 W, they obtained in the simulation the operating frequency as ~2.46 GHz, the peak power as high as >100 kW, high electronic efficiency ~40%, large gain ~50 dB, and tiny size of cross-sectional diameter of only ~40 mm [62]. The above findings clearly show that the novel MTM EIK has prominent advantages such as smaller size, high power, large gain, and high efficiency.

D. MTM-Inspired Accelerators

Antipov *et al.* [63] from the Illinois Institute of Technology, Chicago, IL, USA, and the Argonne National Laboratory, Argonne, IL, investigated the DNM research for accelerator applications in 2007. Their study shows that waveguides loaded with MTMs are of interest due to the DNM changing the dispersion relation of the waveguide significantly. For a typical example, slow backward waves can be produced in a DNM-loaded waveguide without having corrugations.

In 2013, McGregor and Hock [38] from the University of Liverpool, Liverpool, England, proposed a complementary SRR (CSRR)-based deflecting structure for accelerators (Fig. 23). Simulations suggest a total deflecting voltage of 0.132 MV and a transverse accelerating gradient of 1.55 MV/m for only 4.42 kW of applied RF power.

Meanwhile, the waveguide was loaded with another CSRR for accelerator applications [64]. Particle simulation results show that an accelerating gradient of 8.76 MV/m can be obtained in a CSRR-loaded cavity, typically, at 1 GHz for only 10.7 kW of input power [64]. More work can be found, for example, in [65]. A detailed theory of the interaction of an electron beam with an MTM structure has been developed by Lu *et al.* [66]. This work was followed up by an experimental test at the Argonne National Laboratory, where 80 MW of power was generated at 11.4 GHz by an electron bunch traversing a "wagon wheel" MTM structure [67].

III. Discussion Bringing Out Challenges

From the advances in VEDs, we find that an MTM-inspired oscillator/amplifier has a small size, high power, high efficiency, or/and large gain, and an MTM-inspired accelerator has a small size and high accelerating gradient. Therefore, MTMs can really improve the performance of VEDs and accelerators.

A. Difference Between MTM and Periodic Structures

MTM structures enjoy a close relationship with the interaction structures of the VEDs. The first resonant element was possibly the re-entrant cavity used in the klystron [68]. The exciting fact is that the idea of first forming SRRs originated from the concept of the re-entrant klystron cavity. In addition, conventional BWO structures also have some similarities with the novel MTM structures [47], which would attract the VED community.

In the VED community, many researchers believe that an MTM is similar to the periodic structures that are widely used in O-type tubes such as helix and coupled-cavity TWTs. The thinking is true in the sense that an MTM usually consists of periodically arranged unit cells. Moreover, the MTM structures support backward-wave modes as do the conventional SWSs [47]. However, conceptually, the conventional periodic structures are different from the MTM structures in many ways.

First, the theory is different. For MTMs, the effective-medium theory is used. However, for conventional periodic structures, the Floquet's theorem is adopted. Possibly, Floquet's theorem can be used for artificial materials as it is used for MTM structures as well, although the mathematical treatment involved would become very complex. Even more importantly, without the implementation of the MTM concept, it is rather difficult to design the new periodic structure with subwavelength dimensions, which has much higher interaction impedance at S-band [34]. This contribution beyond doubt comes from the emerging MTMs with unusual properties. Thus, the development of the relevant theory taking into account the factors of practical relevance to it becomes very important in the development of the new MTM structures with much higher interaction impedance.

Second, the electromagnetic characteristics of MTMs and conventional periodic structures are different. An MTM structure, for instance, an LHM supports backward waves, while conventional periodic structures can support both forward and backward waves. Most importantly, MTM structures have much higher interaction impedance than the conventional periodic structures owing to the enhanced longitudinal electric field intensity in the former. For instance, while the interaction impedances of helix and CCSWSs are ~100–200 and ~300–400 Ω, respectively, the interaction impedance of a typical MTM SWS could be as high as ~800–1200 Ω. Certainly, this speaks highly of the potential of the MTM structures in VEDs.

Third, the sizes of the conventional periodic and the MTM structures are different. For example, as stated before, the size of the MTM-inspired reversed Cherenkov oscillator is ~1/3–~1/2 of that of the conventional BWO [53]. This miniaturized feature of MTM structures adds to the advantages of the MTM-inspired VEDs. Furthermore, the subwavelength size of an MTM SWS enables one to treat the structure unlike a conventional SWS, but rather as an effective medium characterized by ε_{eff} and μ_{eff}.

B. Challenges

Now that we have appreciated the potential of MTM-inspired VEDs, let us review the various challenges in its research and development.

First, a MTM usually has a strong resonant behavior which results in a very strong dispersion. This implies that MTM-inspired VEDs have a narrow bandwidth. For instance, the tuning bandwidth of the S-band MTM-inspired reversed Cherenkov oscillators developed at UESTC [51] is about 20–30 MHz. Certainly, as far as accelerators are concerned, this is not a problem. This is because the accelerators operate at a single frequency. As a result, MTMs can manifest their advantages for promoting the performance of accelerators. On the contrary, widening the bandwidth of MTM-inspired oscillators and amplifiers is one of the serious challenges needing to be addressed.

Second, loss is an important factor for MTMs to consider. Generally speaking, one has to take into consideration: 1) the ohmic loss (due to resistive heating per unit cell in the metallic layers of the MTM); 2) the dielectric loss including electric and magnetic dielectric loss; and 3) the radiation loss. In the microwave regime, the ohmic loss becomes the main concern [69]. For conventional MTMs consisting of rods and SRRs with a dielectric substrate that works in C-band [4], the transmission coefficient (S_{21}) is ~−30 dB, which corresponds to a loss ~30 dB. Evidently, the loss is rather large and it proves to be a shortcoming of an MTM comprised of rods and SRRs with dielectric substrate. However, the loss of the all-metal (typically, copper) MTM with CeSRRs operating at S-band is ~2 dB. This result is confirmed by both simulation and experiment [9]. In the microwave region, if silver were adapted as a low-loss material to fabricate the MTM, then the loss could be further decreased [70]. Therefore, from the viewpoint of loss, an all-metal MTM is better than a conventional MTM.

Third, the size of the couplers for coupling RF power in and out of SWSs, based on the impedance matching technique, is usually large. Therefore, much work needs to be done in the future, for instance, in the development of MTM-inspired reversed Cherenkov oscillators, to meet the challenge of designing miniaturized RF input–output couplers for them, with the assistance of an MTM [34], [51]–[53].

Fourth, the beam voltage encountered in the design of MTM-inspired VEDs is high. For instance, it is greater than 300 kV in an all-metal MTM-inspired BWO [34]. In order to greatly reduce the beam voltage, a suitable dielectric such as Al_2O_3 or BeO [71] can be embedded into the MTM SWS.

Fifth, an MTM-inspired VED has a smaller beam tunnel relative to its conventional counterpart. This provides lesser room for intense beam current transport for high-power microwave, making the device vulnerable to damage [72].

Finally, the fabrication of MTM-inspired VEDs becomes more and more challenging with the increase of the operating frequency (such as in millimeter wave and THz regimes), more so for bulk MTMs. In addition, the accuracy of processing and assembling will also become more challenging. So, new fabrication technology such as 3-D printing is being attempted [73].

All in all, in view of the advances and challenges in the MTM-inspired VEDs, the research in this type of VEDs has turned out to be an amazing topic in the VED community.

IV. Conclusion

The electromagnetic properties of MTMs (as artificially constructed materials) are controlled by engineering their structure on the subwavelength (microscopic) scale. The rapid development of MTM-related theory and technology provides an unprecedented ability for VED and accelerator designers to manipulate the behavior of the interaction between electromagnetic wave and electron beam/charged particles. From the advances presented here, we see that the MTM-inspired VEDs and accelerators can have significant advantages, such as small size, high power, high efficiency, high gain, or high accelerating gradient, although they are facing serious challenges, too. Therefore, one should accrue the advantages of the MTMs alleviating the shortcomings in the MTM-inspired VEDs and accelerators. In conclusion, this is an emerging research topic in the VED and accelerator areas. Hence, there are many challenges which need to be greatly addressed, not only in physics, but also in technology. We expect more and more researchers worldwide will be involved in these areas for rapidly pushing this brand-new field to a greater height of maturity.

Acknowledgement

Z. Duan would like to thank Prof. N. X. Fang, MIT, for helpful discussions in metamaterials and Prof. M. Chen, MIT, for long-term guidance in RCR.

References

[1] V. G. Veselago, "The electrodynamics of substances with simultaneously negative values of ϵ and μ," *Sov. Phys. Uspekhi*, vol. 47, pp. 509–514, Jan./Feb. 1968, doi: 10.1070/PU1968v010n04ABEH003699.

[2] J. B. Pendry, A. J. Holden, D. J. Robbins, and W. J. Stewart, "Low frequency plasmons in thin-wire structures," *J. Phys., Condens. Matter*, vol. 10, no. 22, pp. 4785–4809, Jun. 1998, doi: 10.1088/0953-8984/28/48/481002.

[3] J. B. Pendry, A. J. Holden, D. J. Robbins, and W. J. Stewart, "Magnetism from conductors and enhanced nonlinear phenomena," *IEEE Trans. Microw. Theory Techn.*, vol. 47, no. 11, pp. 2075–2084, Nov. 1999, doi: 10.1109/22.798002.

[4] D. R. Smith, W. J. Padilla, D. C. Vier, S. C. Nemat-Nasser, and S. Schultz, "Composite medium with simultaneously negative permeability and permittivity," *Phys. Rev. Lett.*, vol. 84, pp. 4184–4187, May 2000, doi: 10.1103/PhysRevLett.84.4184.

[5] R. A. Shelby, D. R. Smith, and S. Schultz, "Experimental verification of a negative index of refraction," *Science*, vol. 292, no. 5514, pp. 77–79, Apr. 2001, doi: 10.1126/science.1058847.

[6] N. Seddon and T. Bearpark, "Observation of the inverse Doppler effect," *Science*, vol. 302, no. 5650, pp. 1537–1540, Nov. 2003, doi: 10.1126/science.1089342.

[7] J. Hummelt, S. Lewis, H. Xu, M. Shapiro, I. Mastovsky, and R. Temkin, "Fabrication and test of a high power S-band metamaterial backward-wave oscillator," in *Proc. IEEE Int. Vac. Electron. Conf. (IVEC)*, Apr. 2015, pp. 1–2, doi: 10.1109/IVEC.2015.7223771.

[8] J. S. Hummelt, X. Lu, H. Xu, I. Mastovsky, M. A. Shapiro, and R. J. Temkin, "Coherent cherenkov-cyclotron radiation excited by an electron beam in a metamaterial waveguide," *Phys. Rev. Lett.*, vol. 117, no. 23, p. 237701, Dec. 2016, doi: 10.1103/PhysRevLett.117.237701.

[9] Z. Duan *et al.*, "Observation of the reversed Cherenkov radiation," *Nature Commun.*, vol. 8, p. 14901, Mar. 2017, doi: 10.1038/ncomms14901.

[10] B. A. Munk, *Metamaterials: Critique and Alternatives*. New York, NY, USA: Wiley, 2009.

[11] N. Engheta and R. W. Ziolkowski, "A positive future for double-negative metamaterials," *IEEE Trans. Microw. Theory Techn.*, vol. 53, no. 4, pp. 1535–1556, Apr. 2005, doi: 10.1109/TMTT.2005.845188.

[12] J. Hodge, T. K. Anthony, and A. I. Zaghloul, "Simulation and analysis of non-periodic and random metamaterial structures," in *Proc. USNC-URSI NRSM*, Boulder, CO, USA, Jan. 2014, pp. 8–11, doi: 10.1109/USNC-URSI-NRSM.2014.6927980.

[13] T. Koschny, M. Kafesaki, E. N. Economou, and C. M. Soukoulis, "Effective medium theory of left-handed materials," *Phys. Rev. Lett.*, vol. 93, no. 10, p. 107402, Sep. 2004, doi: 10.1103/PhysRevLett.93.107402.

[14] D. R. Smith, D. C. Vier, T. Koschny, and C. M. Soukoulis, "Electromagnetic parameter retrieval from inhomogeneous metamaterials," *Phys. Rev. E, Stat. Phys. Plasmas Fluids Relat. Interdiscip. Top.*, vol. 71, pp. 036617-1–036617-11, Mar. 2005, doi: 10.1103/PhysRevE.71.036617.

[15] F. Falcone *et al.*, "Babinet principle applied to the design of metasurfaces and metamaterials," *Phys. Rev. Lett.*, vol. 93, p. 197401, Nov. 2004, doi: 10.1103/PhysRevLett.93.197401.

[16] C. L. Holloway, A. Dienstfrey, E. F. Kuester, J. F. O'Hara, A. K. Azad, and A. J. Taylor, "A discussion on the interpretation and characterization of metafilms/metasurfaces: The two-dimensional equivalent of metamaterials," *Metamaterials*, vol. 3, no. 2, pp. 100–112, Oct. 2009, doi: 10.1016/j.metmat.2009.08.001.

[17] N. Yu *et al.*, "Light propagation with phase discontinuities: Generalized laws of reflection and refraction," *Science*, vol. 334, no. 6054, pp. 333–337, Oct. 2011, doi: 10.1126/science.1210713.

[18] M. Gonidec, "Concept of non-periodic metasurfaces based on positional gradients applied to IR-flat lenses," *Opt. Mater. Express*, vol. 7, no. 7, pp. 2346–2351, Jul. 2017, doi: 10.1364/OME.7.002346.

[19] H.-T. Chen, A. J. Taylor, and N. Yu, "A review of metasurfaces: Physics and applications," *Rep. Prog. Phys.*, vol. 79, no. 7, p. 076401, 2016, doi: 10.1088/0034-4885/79/7/076401.

[20] M. Khorasaninejad and F. Capasso, "Metalenses: Versatile multifunctional photonic components," *Science*, vol. 358, no. 6367, p. 8100, Dec. 2017, doi: 10.1126/science.aam8100.

[21] D. P. Starinshak and J. D. Wilson, "Investigating dielectric and metamaterial effects in a terahertz traveling wave tube amplifier," NASA, Cleveland, OH, USA, Tech. Rep. NASA/TM-2008-215059, 2008.

[22] Z. Duan, B.-I. Wu, J. Lu, J. A. Kong, and M. Chen, "Reversed Cherenkov radiation in unbounded anisotropic double-negative metamaterials," *J. Phys. D, Appl. Phys.*, vol. 42, no. 18, p. 185102, Aug. 2009, doi: 10.1088/0022-3727/42/18/185102.

[23] Z. Duan, B.-I. Wu, S. Xi, H. Chen, and M. Chen, "Research progress in reversed Cherenkov radiation in double-negative metamaterials," *Prog. Electromagn. Res.*, vol. 90, pp. 75–87, 2009, doi: 10.2528/PIER08121604.

[24] Z. Duan, B.-I. Wu, J. Lu, J. A. Kong, and M. Chen, "Cherenkov radiation in anisotropic double-negative metamaterials," *Opt. Express*, vol. 16, no. 22, pp. 18479–18484, Oct. 2008, doi: 10.1364/OE.16.018479.

[25] Z. Duan, B.-I. Wu, J. Lu, J. A. Kong, and M. Chen, "Reversed Cherenkov radiation in a waveguide filled with anisotropic double-negative metamaterials," *J. Appl. Phys.*, vol. 104, no. 6, p. 063303, Sep. 2008, doi: 10.1063/1.2980336.

[26] Y. S. Tan and R. Seviour, "Wave energy amplification in a metamaterial-based traveling-wave structure," *Europhys. Lett.*, vol. 87, no. 3, p. 34005, Aug. 2009, doi: 10.1209/0295-5075/87/34005.

[27] S. K. Datta, L. Kumar, and B. N. Basu, "Investigation into a metamaterial supported helix slow-wave structure," in *Proc. IEEE Int. Vac. Electron. Conf. (IVEC)*, Bangalore, India, Feb. 2011, pp. 211–212, doi: 10.1109/IVEC.2011.5746950.

[28] A. Rashidi and N. Behdad, "Metamaterial-enhanced traveling wave tubes," in *Proc. IEEE Int. Vac. Electron. Conf. (IVEC)*, Monterey, CA, USA, Apr. 2014, pp. 199–200, doi: 10.1109/IVEC.2014.6857559.

[29] A. K. Varshney, R. Guha, S. K. Datta, and B. N. Basu, "Dispersion control of helical slow-wave structure by double-negative metamaterial loading," *J. Electromagn. Waves Appl.*, vol. 30, no. 10, pp. 1308–1320, Jun. 2016, doi: 10.1080/09205071.2016.1198277.

[30] T. Rowe, J. H. Booske, and N. Behdad, "Metamaterial-enhanced resistive wall amplifiers: Theory and particle-in-cell simulations," *IEEE Trans. Plasma Sci.*, vol. 43, no. 7, pp. 2123–2131, Jul. 2015, doi: 10.1109/TPS.2015.2439159.

[31] J. S. Hummelt, S. M. Lewis, M. A. Shapiro, and R. J. Temkin, "Design of a metamaterial-based backward-wave oscillator," *IEEE Trans. Plasma Sci.*, vol. 42, no. 4, pp. 930–936, Apr. 2014, doi: 10.1109/TPS.2014.2309597.

[32] A. Weiss and A. Grbic, "Electron beam coupling to an NRI transmission-line metamaterial," *IEEE Trans. Plasma Sci.*, vol. 43, no. 3, pp. 796–803, Mar. 2015, doi: 10.1109/TPS.2015.2393841.

[33] A. V. Galdetskiy, "On the use of metamaterials for increasing of output power of multibeam klystrons," in *Proc. IEEE Int. Vacuum Electron. Conf. (IVEC)*, Paris, France, May 2013, doi: 10.1109/IVEC.2013.6571125.

[34] Y. Wang *et al.*, "All-metal metamaterial slow-wave structure for high-power sources with high efficiency," *Appl. Phys. Lett.*, vol. 107, no. 15, pp. 153502-1–153502-4, Oct. 2015, doi: 10.1063/1.4933106.

[35] S. C. Yurt, M. I. Fuks, S. Prasad, and E. Schamiloglu, "Design of a metamaterial slow wave structure for an O-type high power microwave generator," *Phys. Plasmas*, vol. 23, no. 12, p. 123115, Dec. 2016, doi: 10.1063/1.4972535.

[36] J. R. Pierce, *Traveling-Wave Tubes*. New York, NY, USA: Van Nostrand, 1950, pp. 390–460, 608-615.

[37] Z. Duan *et al.*, "Review of metamaterial-inspired vacuum electron devices," in *Proc. IEEE Int. Vac. Electron. Conf. (IVEC)*, Monterey, CA, USA, Apr. 2018, pp. 29–30, doi: 10.1109/IVEC.2018.8391536.

[38] I. McGregor and K. M. Hock, "Complementary split-ring resonator-based deflecting structure," *Phys. Rev. ST Accel. Beams*, vol. 16, no. 9, pp. 090101-1–090101-8, Sep. 2013, doi: 10.1103/PhysRevSTAB.16.090101.

[39] Z. Duan, J. S. Hummelt, M. A. Shapiro, and R. J. Temkin, "Subwavelength waveguide loaded by a complementary electric metamaterial for vacuum electron devices," *Phys. Plasmas*, vol. 21, no. 10, pp. 103301-1–103301-6, Oct. 2014, doi: 10.1063/1.4897392.

[40] Z. Duan, C. Guo, and M. Chen, "Enhanced reversed Cherenkov radiation in a waveguide with double-negative metamaterials," *Opt. Express*, vol. 19, no. 15, pp. 13825–13830, Jul. 2011, doi: 10.1364/OE.19.013825.

[41] Z. Duan, C. Guo, J. Zhou, J. Lu, and M. Chen, "Novel electromagnetic radiation in a semi-infinite space filled with a double-negative metamaterial," *Phys. Plasmas*, vol. 19, no. 1, pp. 013112-1–013112-5, Jan. 2012, doi: 10.1063/1.3677888.

[42] Z. Duan, C. Guo, X. Guo, and M. Chen, "Double negative-metamaterial based terahertz radiation excited by a sheet beam bunch," *Phys. Plasmas*, vol. 20, no. 9, pp. 093301-1–093301-6, Sep. 2013, doi: 10.1063/1.4820956.

[43] M. A. Shapiro, S. Trendafilov, Y. Urzhumov, A. Alù, R. J. Temkin, and G. Shvets, "Active negative-index metamaterial powered by an electron beam," *Phys. Rev. B*, vol. 86, no. 8, p. 085132, Aug. 2012, doi: 10.1103/PhysRevB.86.085132.

[44] D. Shiffler, J. Luginsland, D. M. French, and J. Watrous, "A Cerenkov-like maser based on a metamaterial structure," *IEEE Trans. Plasma Sci.*, vol. 38, no. 6, pp. 1462–1465, Jun. 2010, doi: 1109/TPS.2010.2046914.

[45] X. Lu, J. C. Stephens, I. Mastovsky, M. A. Shapiro, and R. J. Temkin, "High power long pulse microwave generation from a metamaterial structure with reverse symmetry," *Phys. Plasmas*, vol. 25, no. 2, p. 023102, Feb. 2018, doi: 10.1063/1.5016545.

[46] M. Buchanan, "Focus: Better microwaves from a metamaterial," *Physics*, vol. 9, p. 141, Dec. 2016, doi: 10.1103/Physics.9.141.

[47] S. C. Yurt, A. Elfrgani, M. I. Fuks, K. Ilyenko, and E. Schamiloglu, "Similarity of properties of metamaterial slow-wave structures and metallic periodic structures," *IEEE Trans. Plasma Sci.*, vol. 44, no. 8, pp. 1280–1286, Aug. 2016, doi: 10.1109/TPS.2016.2535305.

[48] R. Lipton, A. Polizzi, and L. Thakur, "Novel metamaterial surfaces from perfectly conducting subwavelength corrugations," *SIAM J. Appl. Math.*, vol. 77, no. 4, pp. 1269–1291, Aug. 2017, doi: 10.1137/16M109733X.

[49] B. Goplen, L. Ludeking, D. Smith, and G. Warren, "User-configurable MAGIC for electromagnetic PIC calculations," *Comput. Phys. Commun.*, vol. 87, nos. 1–2, pp. 54–86, May 1995, doi: 10.1016/0010-4655(95)00010-D.

[50] S. Prasad *et al.*, "A compact high-power microwave metamaterial slow-wave structure: from computational design to hot test validation," in *Proc. CEIW*, Barcelona, Spain, Jun. 2017, pp. 61–62, doi: 10.1109/CEM.2017.7991887.

[51] Y. Wang *et al.*, "*S*-band high-efficiency metamaterial microwave sources," *IEEE Trans. Electron Devices*, vol. 63, no. 9, pp. 3747–3752, Sep. 2016, doi: 10.1109/TED.2016.2593701.

[52] X. Tang *et al.*, "Sheet electron beam transport in a metamaterial-loaded waveguide under the uniform magnetic focusing," *IEEE Trans. Electron Devices*, vol. 63, no. 5, pp. 2132–2138, May 2016, doi: 10.1109/TED.2016.2544398.

[53] X. Tang *et al.*, "Dual band metamaterial cherenkov oscillator with a waveguide coupler," *IEEE Trans. Electron Devices*, vol. 64, no. 5, pp. 2376–2382, May 2017, doi: 10.1109/TED.2017.2681074.

[54] E. M. Totmeninov, "L-band relativistic traveling wave oscillator based on a circular corrugated waveguide," *IEEE Trans. Plasma Sci.*, vol. 44, no. 8, pp. 1276–1279, Aug. 2016, doi: 10.1109/TPS.2016.2524665.

[55] T. Rowe, N. Behdad, and J. H. Booske, "Metamaterial-enhanced resistive wall amplifier design using periodically spaced inductive meandered lines," *IEEE Trans. Plasma Sci.*, vol. 44, no. 10, pp. 2476–2484, Oct. 2016, doi: 10.1109/TPS.2016.2599144.

[56] T. Rowe, P. Forbes, J. H. Booske, and N. Behdad, "Inductive meandered metal line metamaterial for rectangular waveguide linings," *IEEE. Trans. Plasma Sci.*, vol. 45, no. 4, pp. 654–664, Apr. 2017, doi: 10.1109/TPS.2017.2675706.

[57] R. Guha, A. K. Bandyopadhyay, A. K. Varshney, S. K. Datta, and B. N. Basu, "Investigations into helix slow-wave structure assisted by double-negative metamaterial," *IEEE Trans. Electron Devices*, vol. 65, no. 11, pp. 5082–5088, Nov. 2018, doi: 10.1109/TED.2018.2869831.

[58] S. N. Galyamin, A. V. Tyukhtin, A. Kanareykin, and P. Schoessow, "Reversed Cherenkov-transition radiation by a charge crossing a left-handed medium boundary," *Phys. Rev. Lett.*, vol. 103, no. 19, p. 194802, Nov. 2009, doi: 10.1103/PHYSREVLETT.103.194802.

[59] T. Y. Alekhina and A. V. Tyukhtin, "Reversed Cherenkov-transition radiation in a waveguide partly filled with a left-handed medium," *Radiat. Phys. Chem.*, vol. 145, pp. 43–49, Apr. 2018, doi: 10.1016/j.radphyschem.2017.12.005.

[60] Z. Duan *et al.*, "Recent advances in high-power metamaterial microwave sources at UESTC," in *Proc. IEEE Int. Vac. Electron. Conf. (IVEC)*, London, U.K., Apr. 2017, doi: 10.1109/IVEC.2017.8289567.

[61] T. G. Lee, G. T. Konrad, Y. Okazaki, M. Watanabe, and H. Yonezawa, "The design and performance of a 150-MW klystron at S band," *IEEE Trans. Plasma Sci.*, vol. PS-13, no. 6, pp. 545–552, Dec. 1985, doi: 10.1109/TPS.1985.4316471.

[62] Z. Duan, X. Wang, S. Jiang, Z. Wang, and Y. Gong, "S band metamaterial-based amplifier," in *Proc. IEEE Int. Conf. Plasma Sci. (ICOPS)*, Denver, CO, USA, Jun. 2018.

[63] S. Antipov, L. Spentzouris, W. Gai, W. Liu, and J. G. Power, "Double-negative metamaterial research for accelerator applications," *Nucl. Instrum. Methods Phys. Res. A, Accel. Spectrom. Detect. Assoc. Equip.*, vol. 579, no. 3, pp. 915–923, Sep. 2007, doi: 10.1016/j.nima.2007.04.158.

[64] I. McGregor and K. M. Hock, "Complementary split-ring resonator-based accelerating structure," *J. Instrum.*, vol. 8, p. 05009, May 2013, doi: 10.1088/1748-0221/8/05/P05009.

[65] E. Sharples and R. Letizia, "Investigation of CSRR loaded waveguide for accelerator applications," *J. Instrum.*, vol. 9, p. 11017, Nov. 2014, doi: 10.1088/1748-0221/9/11/P11017.

[66] X. Lu, M. A. Shapiro, and R. J. Temkin, "Modeling of the interaction of a volumetric metallic metamaterial structure with a relativistic electron beam," *Phys. Rev. Accel. Beams*, vol. 18, no. 8, p. 081303, Aug. 2015, doi: 10.1103/PhysRevSTAB.18.081303.

[67] X. Lu *et al.*, "A metamaterial wagon wheel structure for wakefield acceleration by reversed cherenkov radiation," in *Proc. 9th Int. Part. Accel. Conf. (IPAC)*, Vancouver, BC, Canada, 2018, pp. 4681–4683.
[68] W. W. Hansen and R. D. Richtmyer, "On resonators suitable for klystron oscillators," *J. Appl. Phys.*, vol. 10, no. 3, pp. 189–199, Mar. 1939, doi: 10.1063/1.1707295.
[69] T. Koschny, J. Zhou, and C. M. Soukoulis, "Magnetic response and negative refractive index of metamaterials," in *Proc. SPIE*, vol. 6581, p. 658103, May 2007, doi: 10.1117/12.724176.
[70] G. Dolling, C. Enkrich, M. Wegener, C. M. Soukoulis, and S. Linden, "Low-loss negative-index metamaterial at telecommunication wavelengths," *Opt. Lett.*, vol. 31, no. 12, pp. 1800–1802, Jun. 2006, doi: 10.1364/OL.31.001800.
[71] J. G. Power *et al.*, "Observation of multipactor in an alumina-based dielectric-loaded accelerating structure," *Phys. Rev. Lett.*, vol. 92, no. 16, p. 164801, Apr. 2004, doi: 10.1103/PhysRevLett.92.164801.
[72] J. H. Booske, "Plasma physics and related challenges of millimeter-wave-to-terahertz and high power microwave generation," *Phys. Plasmas*, vol. 15, no. 5, pp. 055502-1–055502-16, May 2008, doi: 10.1063/1.2838240.
[73] D. M. French and D. Shiffler, "High power microwave source with a three dimensional printed metamaterial slow-wave structure," *Appl. Phys. Lett.*, vol. 87, no. 5, p. 053308, May 2016, doi: 10.1063/1.4950904.

Zhaoyun Duan (M'06–SM'10) received the Ph.D. degree in physical electronics from the University of Electronic Science and Technology of China (UESTC), Chengdu, China, in 2004.

He is currently a Full Professor and serves as the Deputy Dean of the School of Electronic Science and Engineering, UESTC.

Dr. Duan is an IET Fellow.

Michael A. Shapiro (M'09–SM'17) received the Ph.D. degree in radio physics from Gorky State University, Gorky, Russia, in 1990.

He has been with the Plasma Science and Fusion Center, Massachusetts Institute of Technology, Cambridge, MA, USA, since 1995, where he is currently the Head of the Gyrotron Research Group.

Edl Schamiloglu (M'90–SM'95–F'02) received the B.S. and M.S. degrees from Columbia University SEAS, New York City, NY, USA, in 1979 and 1981, respectively, and the Ph.D. degree in engineering from Cornell University, Ithaca, NY, USA, in 1988.

He is currently a Distinguished Professor of electrical engineering with the University of New Mexico, Albuquerque, NM, USA.

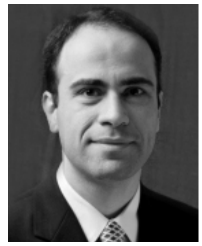

Nader Behdad (S'98–M'06–SM'12–F'17) is currently a Professor and an H. D. Spangler Scholar with the Electrical and Computer Engineering Department, University of Wisconsin–Madison, Madison, WI, USA. His current research interests include antennas, metamaterials, high-power microwaves, and microwave medical applications.

Yubin Gong (M'02) received the Ph.D. degree in physical electronics from the University of Electronic Science and Technology of China (UESTC), Chengdu, China, in 1998.

He is currently a Full Professor and serves as the Deputy Director of the National Key Laboratory of Science and Technology on Vacuum Electronics.

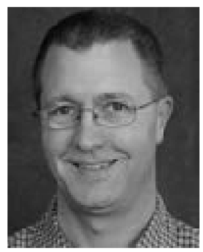

John H. Booske (S'82–M'85–SM'93–F'07) is currently a Professor with the Electrical and Computer Engineering Department, University of Wisconsin–Madison, Madison, WI, USA. His current research interests include RF-to-THz radiation sources and applications, including vacuum electronics, plasmas, and biological applications of electric and electromagnetic fields.

B. N. Basu (M'18) received the Ph.D. degree in radiophysics and electronics from Calcutta University, Kolkata, India, in 1976.

He was a Professor and the Head of Electronics Engineering Department, IIT-BHU, Varanasi, India.

Richard J. Temkin (M'87–SM'92–F'94–LF'17) received the B.A. degree from Harvard College, Cambridge, MA, USA, and the Ph.D. degree from Massachusetts Institute of Technology (MIT), Cambridge, in 1966 and 1971, respectively.

He is currently a Senior Scientist in physics and the Associate Director of the Plasma Science and Fusion Center, MIT.

Dr. Temkin is a fellow of APS and IoP.